Molecularly Ordered Ethylene-Bridged Periodic Mesoporous Organosilica Spheres with Tunable Micrometer Sizes

Yongde Xia, Zhuxian Yang, and Robert Mokaya*

School of Chemistry, University of Nottingham, Nottingham, NG7 2RD, United Kingdom

Received December 1, 2005. Revised Manuscript Received January 18, 2006

We report the synthesis of periodic mesoporous organosilica (PMO) spheres of a size between 3 and 14 μm. The ethylene-bridged PMO spheres were prepared via surfactant (dodecyltrimethylammonium bromide) mediated assembly of 1,2-bis(triethoxysilyl)ethylene without using any additional cosolvents and/or cosurfactants. The PMO spheres exhibit molecular-scale ordering with a periodicity of 5.6 Å due to a crystal-like arrangement of the ethylene groups in the organosilica framework. The morphology (i.e., formation of spheres) and level of mesostructural ordering in the PMO materials were dependent on the basicity of the synthesis media, while the size of the relatively monodisperse spheres was readily controlled by variations in the concentration of surfactant. The PMO materials are mesostructurally well-ordered and exhibit a high surface area (>900 m^2/g) and pore volume (>0.8 cm^3/g). The molecularly ordered ethylene groups within the organosilica framework were found to present a versatile and reactive functionality as demonstrated by bromination of the PMO spheres.

Introduction

In the past decade, mesostructured silica-based inorganic materials prepared via supramolecular assembly have attracted intense interest due to their potential use in a wide range of applications.[1,2] Mesostructured silica-based materials are typically prepared via surfactant mediated self-assembly of suitable silica precursors.[1,2] Materials with various particle morphology, including fibers, rods, tubes, films, monoliths, spheres, and hollow spheres have been fabricated using a variety of surfactants and silica precursors.[2] In particular, monodisperse spherical particles of micrometer sizes that exhibit high surface area, high pore volume, and narrow pore size distribution are attractive for many applications such as in drug delivery, multifunctional catalysis, macromolecule separations, photonic crystals,[2,3] and, in particular, for chromatographic applications.[4] Monodisperse mesostructured spherical particles have been prepared from both acidic and basic media using a variety of surfactants and silica precursors.[5−8] In most cases, however, an additional cosolvent and/or cosurfactant is necessary to control the morphology toward the formation of spheres.[7,8]

Purely siliceous materials, however, have limitations with respect to their poor mechanical properties and limited range of surface functionalities. Therefore, the introduction of organic moieties into structurally well-ordered mesoporous silica materials is an attractive theme in nanomaterial research.[9] Specifically, mesoporous organosilica materials with a homogeneous distribution of organic species both in

* Corresponding author. E-mail: r.mokaya@nottingham.ac.uk.

(1) (a) Davis, M. E. *Nature* **2002**, *417*, 813. (b) Ying, J. Y.; Mehnert, C. P.; Wong, M. S. *Angew. Chem., Int. Ed. Engl.* **1999**, *38*, 56. (c) Corma, A. *Chem. Rev.* **1997**, *97*, 2373.

(2) (a) Stein, A. *Adv. Mater.* **2003**, *15*, 763. (b) Lin, H. P.; Mou, C. Y. *Acc. Chem. Res.* **2002**, *35*, 927. (c) Schuth, F.; Schmidt, W. *Adv. Mater.* **2002**, *14*, 629. (d) Yang, H. F.; Zhao, D. Y. *J. Mater. Chem.* **2005**, *15*, 1217. (e) On, D. T.; Desplantier-Giscard, D.; Danumah, C.; Kaliaguine, S. *Appl. Catal., A* **2001**, *222*, 299. (f) Yang, H.; Coombs, N.; Ozin, G. A. *Nature* **1997**, *386*, 692.

(3) Yang, H. F.; Yan, Y.; Zhao, D. Y. *J. Ind. Eng. Chem.* **2004**, *10*, 1146.

(4) (a) Martin, T.; Galarneau, A.; Di Renzo, F.; Brunel, D.; Fajula, F.; Heinisch, S.; Cretier, G.; Rocca, J. L. *Chem. Mater.* **2004**, *16*, 1725. (b) Salesch, T.; Bachmann, S.; Brugger, S.; Rabelo-Schaefer, R.; Albert, K.; Steinbrecher, S.; Plies, E.; Mehdi, A.; Reye, C.; Corriu, R. J. P.; Lindner, E. *Adv. Funct. Mater.* **2002**, *12*, 134. (c) Boissiere, C.; Kummel, M.; Persin, M.; Larbot, A.; Prouzet, E. *Adv. Funct. Mater.* **2001**, *11*, 129. (d) Ma, Y. R.; Qi, L. M.; Ma, J. M.; Wu, Y. Q.; Liu, O.; Cheng, H. M. *Colloids Surf., A* **2003**, *229*, 1. (e) Gallis, K. W.; Araujo, J. T.; Duff, K. J.; Moore, J. G.; Landry, C. C. *Adv. Mater.* **1999**, *11*, 1452.

(5) (a) Rao, G. V. R.; Lopez, G. P.; Bravo, J.; Pham, H.; Datye, A. K.; Xu, H. F.; Ward, T. L. *Adv. Mater.* **2002**, *14*, 1301. (b) Kosuge, K.; Murakami, T.; Kikukawa, N.; Takemori, M. *Chem. Mater.* **2003**, *15*, 3184. (c) Kosuge, K.; Kikukawa, N.; Takemori, M. *Chem. Mater.* **2004**, *16*, 4181. (d) Kosuge, K.; Singh, P. S. *Chem. Mater.* **2001**, *13*, 2476. (e) Yang, H.; Vovk, G.; Coombs, N.; Sokolov, I.; Ozin, G. A. *J. Mater. Chem.* **1998**, *8*, 743.

(6) (a) Petitto, C.; Galarneau, A.; Driole, M. F.; Chiche, B.; Alonso, B.; Di Renzo, F.; Fajula, F. *Chem. Mater.* **2005**, *17*, 2120. (b) Chen, C. N.; Lin, H. P.; Tsai, C. P.; Tang, C. Y. *Chem. Lett.* **2004**, *33*, 838. (c) Fowler, C. E.; Khushalani, D.; Lebeau, B.; Mann, S. *Adv. Mater.* **2001**, *13*, 649. (d) Cai, Q.; Luo, Z. S.; Pang, W. Q.; Fan, Y. W.; Chen, X. H.; Cui, F. Z. *Chem. Mater.* **2001**, *13*, 258. (e) Huo, Q. S.; Feng, J. L.; Schuth, F.; Stucky, G. D. *Chem. Mater.* **1997**, *9*, 14.

(7) (a) Schumacher, K.; Du Fresne von Hohenesche, C.; Unger, K. K.; Ulrich, R.; Du Chesne, A.; Wiesner, U.; Spiess, H. W. *Adv. Mater.* **1999**, *11*, 1194. (b) Buechel, G.; Unger, K. K.; Matsumoto, A.; Tsutsumi, K. *Adv. Mater.* **1998**, *10*, 1036 (c) Gruen, M.; Lauer, I.; Unger, K. K. *Adv. Mater.* **1997**, *9*, 254.

(8) (a) Martin, T.; Galarneau, A.; Di Renzo, F.; Fajula, F.; Plee, D. *Angew. Chem., Int. Ed.* **2002**, *41*, 2590. (b) Lefevre, B.; Galarneau, A.; Iapichella, J.; Petitto, C.; Di Renzo, F.; Fajula, F.; Bayram-Hahn, Z.; Skudas, R.; Unger, K. *Chem. Mater.* **2005**, *17*, 601. (c) Yano, K.; Fukushima, Y. *J. Mater. Chem.* **2004**, *14*, 1579. (d) Zhang, Y. B.; Qian, X. F.; Li, Z. K.; Yin, J.; Zhu, Z. K. *J. Solid State Chem.* **2004**, *177*, 844. (e) Nooney, R. I.; Thirunavukkarasu, D.; Chen, Y. M.; Josephs, R.; Ostafin, A. E. *Chem. Mater.* **2002**, *14*, 4721. (f) Zhao, D. Y.; Sun, J. Y.; Li, Q. Z.; Stucky, G. D. *Chem. Mater.* **2000**, *12*, 275. (g) Boissiere, C.; van der Lee, A.; El Mansouri, A.; Larbot, A.; Prouzet, E. *Chem. Commun.* **1999**, 2047.

(9) (a) Hatton, B.; Landskron, K.; Whitnall, W.; Perovic, D.; Ozin, G. A. *Acc. Chem. Res.* **2005**, *38*, 305. (b) Sanchez, C.; Lebeau, B.; Chaput, F.; Boilot, J. P. *Adv. Mater.* **2003**, *15*, 1969. (c) Wight, A. P.; Davis, M. E. *Chem. Rev.* **2002**, *102*, 3589. (d) Sayari, A.; Hamoudi, S. *Chem. Mater.* **2001**, *13*, 3151. (e) Stein, A.; Melde, B. J.; Schroden, R. C. *Adv. Mater.* **2000**, *12*, 1403.

10.1021/cm0526563 CCC: $33.50
Published on Web 02/10/2006

the pore wall framework and on the pore wall surface are fascinating from both a materials and chemistry point of view.[9] Various organic moieties, including methylene, ethane, ethylene, thiophene, allyl, phenyl, biphenyl, two- or three-substituted phenyl, large heterocyclic groups, and three-ring precursors, have been uniformly incorporated into the pore walls of so-called periodic mesoporous organosilica (PMO) materials.[10−12] Phenyl, biphenyl, ethylene, and allyl-containing PMOs have been found to exhibit molecular-scale periodicity in their pore walls.[11] To date, there are, however, very few reports on the synthesis of spherical PMO materials;[13] Ethane-, phenyl-, and ethylene-containing mesostructured organosilica spheres have been fabricated via modified Stöber methods in the presence of ethanol,[13] but so far, no molecular scale ordering has been achieved in any spherical PMO.[4−8,13]

One of the most exciting potential applications of spherical PMOs is as a stationary phase in liquid-phase chromatography. A limiting factor in this regard is sphere size; to use spherical mesoporous silica in liquid-phase chromatography,[4] it is desirable that the spheres be monodispersed and of a size no lower than 2−3 μm so as to allow easy packing and reduce hydrodynamic energy costs.[4a,4c] With no exception, all mesoporous organosilica spheres that have been reported to date are smaller than 2 μm and typically between 0.2 and 1 μm.[13] This is perhaps due to the fact that, in most cases, sphere size is difficult to control for both silica and organosilica materials.[4−8,13] Easy control of PMO sphere size is therefore a desirable research goal that has so far not been achieved. Apart from a controllable sphere size, it is also desirable that PMOs have organosilica frameworks that are amenable to further functionalization by way of reactive organo groups. Ethylene is a versatile reactive organic group that can be readily subjected to various chemical modifications.[10a,10c,12c,13c] Furthermore, molecularly ordered ethylene groups would present advantages with respect to the arrangement of functional groups. It is therefore highly desirable to demonstrate the fabrication of ethylene-bridged spherical mesoporous organosilica materials that possess monodisperse spheres of controllable size in the micrometer range. Here, we report the synthesis of structurally well-ordered ethylene-bridged mesoporous organosilica materials, which exhibit molecular-level periodicity in their pore walls and spherical particle morphology with spheres of a tunable micrometer size. We show that the morphology, structural ordering, and sphere size of the PMO materials can be readily adjusted by controlling the basicity and/or the concentration of surfactant during synthesis and that the presence of ethylene groups offers opportunities for further functionalization via simple chemical reactions.

Experimental Procedures

Material Synthesis. 1,2-bis(Triethoxysilyl)ethylene (BTEE) was synthesized following an established procedure.[14] Only the distilled fraction with a boiling point higher than 90 °C/15 μm Hg was used. The synthesis procedure for the organosilica materials was as follows: a calculated amount of dodecyltrimethylammonium bromide (DTAB) was dissolved in 64.87 g of distilled water under stirring, followed by the addition of NaOH to control the pH. A total of 3.52 g of BTEE was then added to the mixture with stirring to give a gel mixture of molar ratio 1 BTEE/0.6−1.6 DTAB/1.6−2.4 NaOH/360 H_2O. After continuously stirring for 20 h at room temperature, the synthesis gel mixture was transferred to an autoclave and aged at 100 °C for 24 h. The autoclave was then cooled to room temperature, and the solid product was obtained by filtration and repeatedly washed with a large amount of distilled water. After air-drying at room temperature, the dry (as-synthesized) material was subjected to refluxing in an ethanol solution containing 4 wt % HCl for 2 h to extract the DTAB surfactant. The solvent extraction procedure was repeated 3 times to ensure complete removal of the surfactant. Organosilica samples (prepared at a H_2O/DTAB molar ratio of 300) were labeled as EHOI-A, -B, -C, -D, and -E for H_2O/NaOH molar ratio of 225, 200, 180, 163.6, and 150, respectively. Two further samples (designated as EHOI-F and -G) were prepared at a H_2O/DTAB molar ratio of 600 and 225, respectively, and a H_2O/NaOH molar ratio of 150.

Bromination. The reactivity of the ethylene groups was probed using the bromination reaction as follows: 0.2 g of surfactant-free organosilica material (EHOI-C sample) was predried at 100 °C for several hours and loaded into a small glass vial, which was placed in a glass beaker. Several drops of bromine were added to the beaker, avoiding direct contact with the organosilica sample in the vial. The beaker was covered with Parafilm to contain the bromine gas, and the organosilica sample was exposed to bromine for a period of 24 h at room temperature. The brominated organosilica sample (designated BEHOI-C) was then washed with dichloromethane (CH_2Cl_2), followed by further washing with a large amount of water and ethanol. The color of the product changed from orange to white during the washing procedure, implying the complete removal of any physisorbed bromine.[10c]

Material Characterization. Powder X-ray diffraction (XRD) analysis was performed using a Philips 1830 powder diffractometer with Cu Kα radiation (40 kV, 40 mA). Scanning electron microscopy (SEM) images were recorded using a JEOL JSM-820

(10) (a) Asefa, T.; MacLachlan, M. J.; Coombs, N.; Ozin, G. A. *Nature* **1999**, *402*, 867. (b) Inagaki, S.; Guan, S.; Fukushima, Y.; Ohsuna, T.; Terasaki, O. *J. Am. Chem. Soc.* **1999**, *121*, 9611. (c) Melde, B. J.; Holland, B. T.; Blanford, C. F.; Stein, A. *Chem. Mater.* **1999**, *11*, 3302.

(11) (a) Inagaki, S.; Guan, S.; Ohsuna, T.; Terasaki, O. *Nature* **2002**, *416*, 304. (b) Kapoor, M. P.; Inagaki, S.; Ikeda, S.; Kakiuchi, K.; Suda, M.; Shimada, T. *J. Am. Chem. Soc.* **2005**, *127*, 8174. (c) Kapoor, M. P.; Yang, Q.; Inagaki, S. *Chem. Mater.* **2004**, *16*, 1209. (d) Kapoor, M. P.; Yang, Q.; Inagaki, S. *J. Am. Chem. Soc.* **2002**, *124*, 15176. (e) Yang, Q.; Kapoor, M. P.; Inagaki, S. *J. Am. Chem. Soc.* **2002**, *124*, 9694. (f) Xia, Y. D.; Wang, W. X.; Mokaya, R. *J. Am. Chem. Soc.* **2005**, *127*, 790. (g) Xia, Y. D.; Mokaya, R. *J. Mater. Chem.* **2006**, *16*, 395. (h) Sayari, A.; Wang, W. *J. Am. Chem. Soc.* **2005**, *127*, 12194.

(12) (a) Olkhovyk, O.; Jaroniec, M. *J. Am. Chem. Soc.* **2005**, *127*, 60. (b) Morell, J.; Wolter, G.; Froba, M. *Chem. Mater.* **2005**, *17*, 804. (c) Wang, W. H.; Xie, S. H.; Zhou, W. Z.; Sayari, A. *Chem. Mater.* **2004**, *16*, 1756. (d) Wang, W.; Zhou, W.; Sayari, A. *Chem. Mater.* **2003**, *15*, 4886. (e) Landskron, K.; Hatton, B. D.; Perovic, D. D.; Ozin, G. A. *Science* **2003**, *302*, 266. (f) Goto, Y.; Inagaki, S. *Chem. Commun.* **2002**, 2410. (g) Asefa, T.; Kruk, M.; MacLachlan, M. J.; Coombs, N.; Grondey, H.; Jaroniec, M.; Ozin, G. A. *J. Am. Chem. Soc.* **2001**, *123*, 8520. (h) Dag, O.; Yoshina-Ishii, C.; Asefa, T.; MacLachlan, M. J.; Grondey, H.; Coombs, N.; Ozin, G. A. *Adv. Funct. Mater.* **2001**, *11*, 213. (i) Lu, Y.; Fan, H.; Doke, N.; Loy, D. A.; Assink, R. A.; LaVan, D. A.; Brinker, C. J. *J. Am. Chem. Soc.* **2000**, *122*, 5258. (j) Guan, S.; Inagaki, S.; Ohsuna, T.; Terasaki, O. *J. Am. Chem. Soc.* **2000**, *122*, 5660. (k) Sayari, A.; Hamoudi, S.; Yang, Y.; Moudrakovski, I. L.; Ripmeester, J. R. *Chem. Mater.* **2000**, *12*, 3857.

(13) (a) Rebbin, V.; Jakubowski, M.; Potz, S.; Froba, M. *Microporous Mesoporous Mater.* **2004**, *72*, 99. (b) Kapoor, M. P.; Inagaki, S. *Chem. Lett.* **2004**, *33*, 88. (c) Xia, Y.; Mokaya, R. *Microporous Mesoporous Mater.* **2005**, *86*, 231.

(14) Loy, D. A.; Carpenter, J. P.; Yamanaka, S. A.; McClain, M. D.; Greaves, J.; Hobson, S.; Shea, K. J. *Chem. Mater.* **1998**, *10*, 4129.

Table 1. Textural Properties of Surfactant-Free Spherical Mesoporous Organosilica Materials

sample	H_2O/NaOH molar ratio	H_2O/DTAB molar ratio	surface area [$m^2\ g^{-1}$]	pore volume [$cm^3\ g^{-1}$]	pore size[a] [Å]
EHOI-A	225	300	970	0.90	20.8
EHOI-B	200	300	978	0.99	21.0
EHOI-C	180	300	942	0.91	22.7
BEHOI-C[b]			776	0.71	20.6
EHOI-D	163.6	300	959	0.84	20.0
EHOI-E	150	300	940	0.83	22.6
EHOI-F	150	600	944	0.83	20.0
EHOI-G	150	225	1006	0.88	20.9

[a] Average pore size calculated using BJH analysis of nitrogen adsorption isotherm. [b] Brominated sample.

scanning electron microscope. Transmission electron microscopy (TEM) images were recorded on a JEOL 2000-FX electron microscope operating at 200 kV. Nitrogen sorption isotherms and textural properties of the materials were determined at −196 °C using nitrogen in a conventional volumetric technique by a Micromeritics ASAP 2020 sorptometer. Before analysis, the samples were oven dried at 150 °C and evacuated for 12 h at 200 °C under vacuum. The surface area was calculated using the BET method based on adsorption data in the partial pressure (P/P_0) range of 0.05−0.2, and a total pore volume was determined from the amount of the nitrogen adsorbed at P/P_0 = ca. 0.99. The average pore size was calculated using BJH analysis of the adsorption isotherm. ^{29}Si and ^{13}C magic angle spinning (MAS) nuclear magnetic resonance (NMR) spectra were acquired at the EPSRC Solid-State NMR Service (Durham, UK) on a Varian Unity Inova 300 MHz spectrometer using a 7.5 mm probe. ^{29}Si spectra were obtained with a Si-29 frequency of 59.55 MHz, spectral width of 30 kHz, acquisition time of 30 ms, and MAS rate of 5.1 kHz. ^{13}C spectra were obtained using a cross polarization experiment at a frequency of 75.39 MHz, spectral width of 30 kHz with an acquisition time of 20 ms, and MAS rate of 5.0 kHz. ^{29}Si and ^{13}C signals were referenced to tetramethylsilane (TMS).

Results and Discussion

Formation of PMO Spheres and Control of Sphere Size. The particle morphology of organosilica materials, prepared at various basicities (i.e., pH values determined by H_2O/NaOH ratios as given in Table 1), is shown by the SEM images in Figure 1. Materials synthesized at a H_2O/NaOH molar ratio ≤180 exclusively exhibit spherical particle morphology (Figure 1A−D). The spheres have smooth surfaces and sizes typically in the range of 6−9 μm (Figure 1A−D). At lower basicity (H_2O/NaOH molar ratio of 200), the formation of spheres is less predominant (Figure 1E), and hardly any spheres are formed at the lowest basicity (H_2O/NaOH molar ratio of 225) as shown in Figure 1F. Remarkably, for samples (EHOI-C, -D, and -E) prepared at H_2O/NaOH molar ratios of between 150 and 180, virtually all the spheres formed are free-standing without aggregation. Furthermore, the basicity does not appear to have any influence on the size (6−9 μm) of these well-formed and free-standing spheres.

Most practical applications of spherical materials require that the sphere size be readily controlled. We studied the influence of surfactant (DTAB) concentration on the size of the organosilica spheres; Figure 2 shows SEM images of materials prepared at H_2O/NaOH ratios of 150 and H_2O/DTAB molar ratios of 600, 300, or 225. The SEM images indicate a gradual decrease in sphere size at higher concentrations (low dilution) of surfactant. We found that low DTAB concentrations (H_2O/DTAB molar ratio of 600) generated spheres (sample EHOI-F) of sizes in the range of 7.5−12 μm (Figure 2A,B). An increase in the DTAB concentration (H_2O/DTAB molar ratio of 300, sample EHOI-E) resulted in spheres of sizes of 5.0−8 μm. Further increases in the surfactant concentration (sample EHOI-G, H_2O/DTAB molar ratio of 225) resulted in a decrease of sphere sizes to between 3.0 and 4.5 μm. In all three cases, the spheres are well-formed and free-standing.

It is worth noting that the present ethylene-bridged organosilica spheres were synthesized without using any cosolvent and/or cosurfactant. We believe this was possible because of the high basicity of the synthesis mixtures and the hydrophilic properties of the DTAB surfactant in aqueous solution as compared with other long-chain alkyltrimethylammonium surfactants.[6b] The hydrophilicity of the surfactant is determined by the alkyl chain length and nature (polarity) of the solvent. The high basicity of the synthesis mixtures (for H_2O/NaOH ratios between 150 and 180) and hydrophilicity of the DTAB surfactant prevented rapid silicate-surfactant precipitation (i.e., the formation of heterogeneous particle shapes with a broad size distribution was inhibited), thus allowing relatively monodisperse spheres to be generated.

Structural Ordering, Molecular Ordering, and Porosity of Spherical PMOs. The structural ordering of the organosilica materials was evaluated by powder X-ray diffraction (XRD). Figure 3 shows the XRD patterns of surfactant-free organosilica samples synthesized at various pH values (H_2O/NaOH ratios). The low-angle region of the XRD patterns (Supporting Information Figure 1S) indicates varying levels of structural ordering, ranging from patterns typical of highly ordered MCM-41 type structures (samples EHOI-B and -C) to less well-ordered materials (samples EHOI-A and -D). The XRD pattern of sample EHOI-E (not shown) is similar to that of sample EHOI-D. The XRD patterns of samples prepared at H_2O/NaOH ratios of 180 and 200 (samples EHOI-B and -C) exhibit an intense basal (100) diffraction peak and two well-resolved higher order peaks in the 2θ range of 3−6°, which can be attributed to (110) and (200) diffractions of a two-dimensional *P6mm* hexagonal structure.[15] The XRD patterns of the other samples show diffuse basal peaks, suggesting lower levels of mesostructural ordering. It is therefore clear that intermediate basicity conditions (H_2O/NaOH molar ratios in the range of 180−200; samples EHOI-B and -C) generate structurally highly ordered materials. When the basicity is too low (sample EHOI-A) or too high (sample EHOI-D and -E), the mesostructural ordering is compromised. The basal spacing obtained from the XRD patterns (36.5, 39.6, and 37.8 Å for samples EHOI-A, -B, and -C, respectively) is comparable

(15) (a) Kresge, C. T.; Leonowicz, M. E.; Roth, W. J.; Vartuli, J. C.; Beck, J. S. *Nature* **1992**, *359*, 710. (b) Beck, J. S.; Vartuli, J. C.; Roth, W. J.; Leonowicz, M. E.; Kresge, C. T.; Schmitt, K. D.; Chu, C. T.-W.; Olson, D. H.; Sheppard, E. W.; McCullen, S. B.; Higgins, J. B.; Schlenker, J. L. *J. Am. Chem. Soc.* **1992**, *114*, 10834.

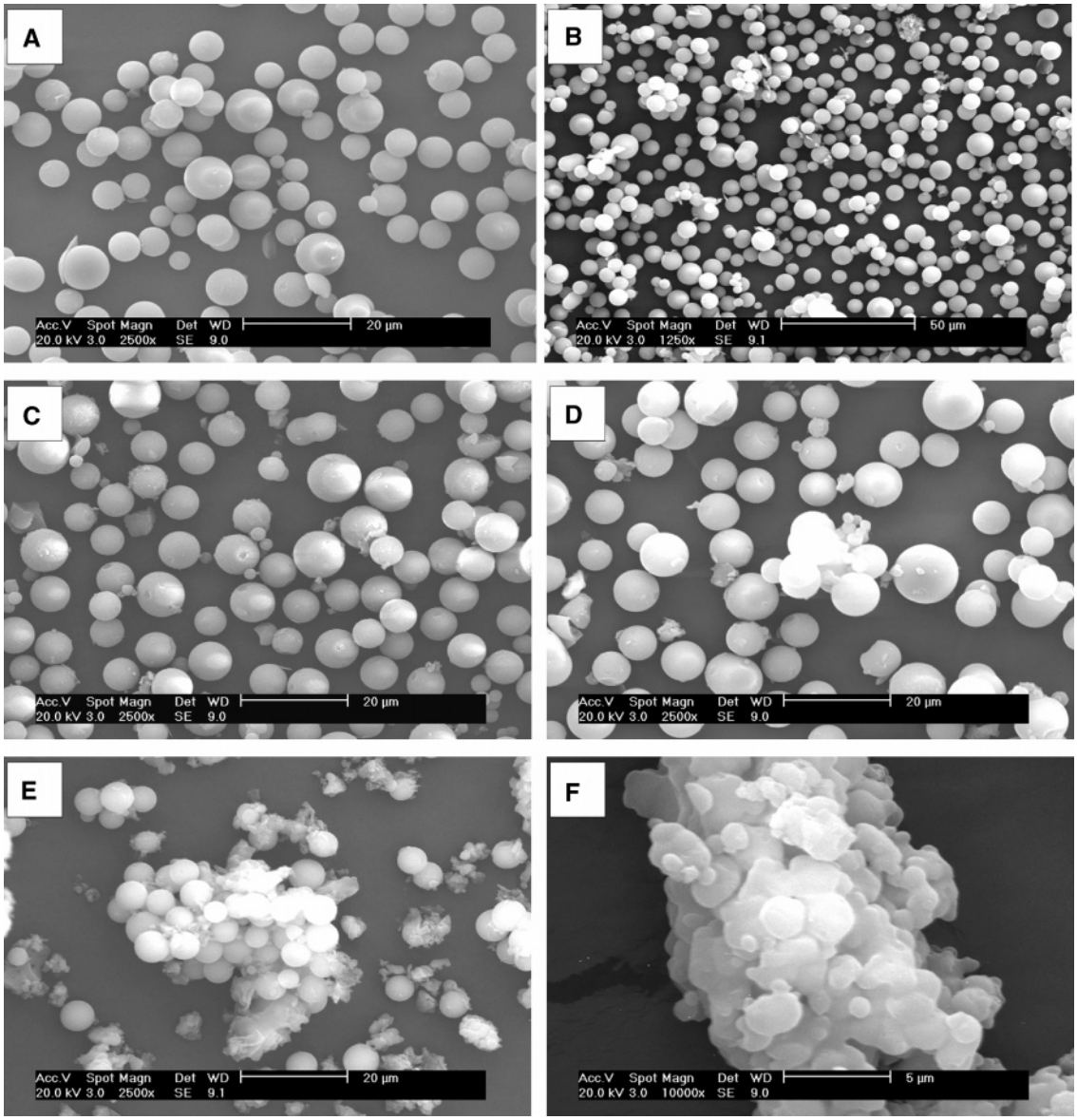

Figure 1. Representative SEM images of ethylene-bridged organosilica materials prepared at a H_2O/DTAB molar ratio of 300 and varying basicity at a H_2O/NaOH molar ratio of (A and B) 150, (C) 163.6, (D) 180, (E) 200, and (F) 225.

for all PMOs. This suggests that the basicity of the synthesis mixtures does not have a significant influence on the basal spacing.

In addition to the low-angle XRD peaks, all the samples exhibit a further peak at $2\theta = 16.5°$ (i.e., at a basal spacing of 5.6 Å) arising from molecular-scale ordering of the ethylene groups within the organosilica framework.[11b] The intensity of this peak, for the various samples, suggests that the materials have comparable levels of molecular ordering. This implies that the basicity range used in our synthesis conditions had no significant influence on the molecular scale periodicity of ethylene groups. This is the first time that molecularly ordered PMO spheres have been achieved. We believe that appropriately basic conditions (i.e., pH $\geq$ 12) are necessary for the formation of molecularly ordered ethylene-bridged PMOs. We have previously prepared small PMO spheres (of sizes 0.5−1.0 μm) in the presence of ethanol and under weakly basic media (pH of ca. 8−10) and observed no molecular ordering.[13c] Furthermore, Sayari and co-workers observed no molecular scale periodicity for ethylene-containing PMOs that were prepared under acidic conditions.[12c] Our observations therefore emphasize the importance of using the optimum synthesis conditions (with respect to pH, nature, and amount of surfactant) in generating large (>2 μm) PMO spheres that possess molecular scale periodicity.

The nitrogen sorption isotherms of the organosilica materials are presented in Figure 4, and the corresponding textural properties are summarized in Table 1. The materials exhibit type IV isotherms with a typical capillary condensation step into mesopores. All the isotherms exhibit type H2 hysteresis, which we ascribe to network effects commonly observed for this type of material.[16] The average pore size estimated from BJH analysis of the adsorption branch of the isotherms varies between 20 and 23 Å (Table 1). (We note that the estimated average pore size is dependent on the method used to calculate the pore size. The adsorption rather than desorption

(16) (a) Kruk, M.; Jaroniec, M. *Chem. Mater.* **2001**, *13*, 3169. (b) Tompsett, G. A.; Krogh, L.; Griffin, D. W.; Conner, W. C. *Langmuir* **2005**, *21*, 8214.

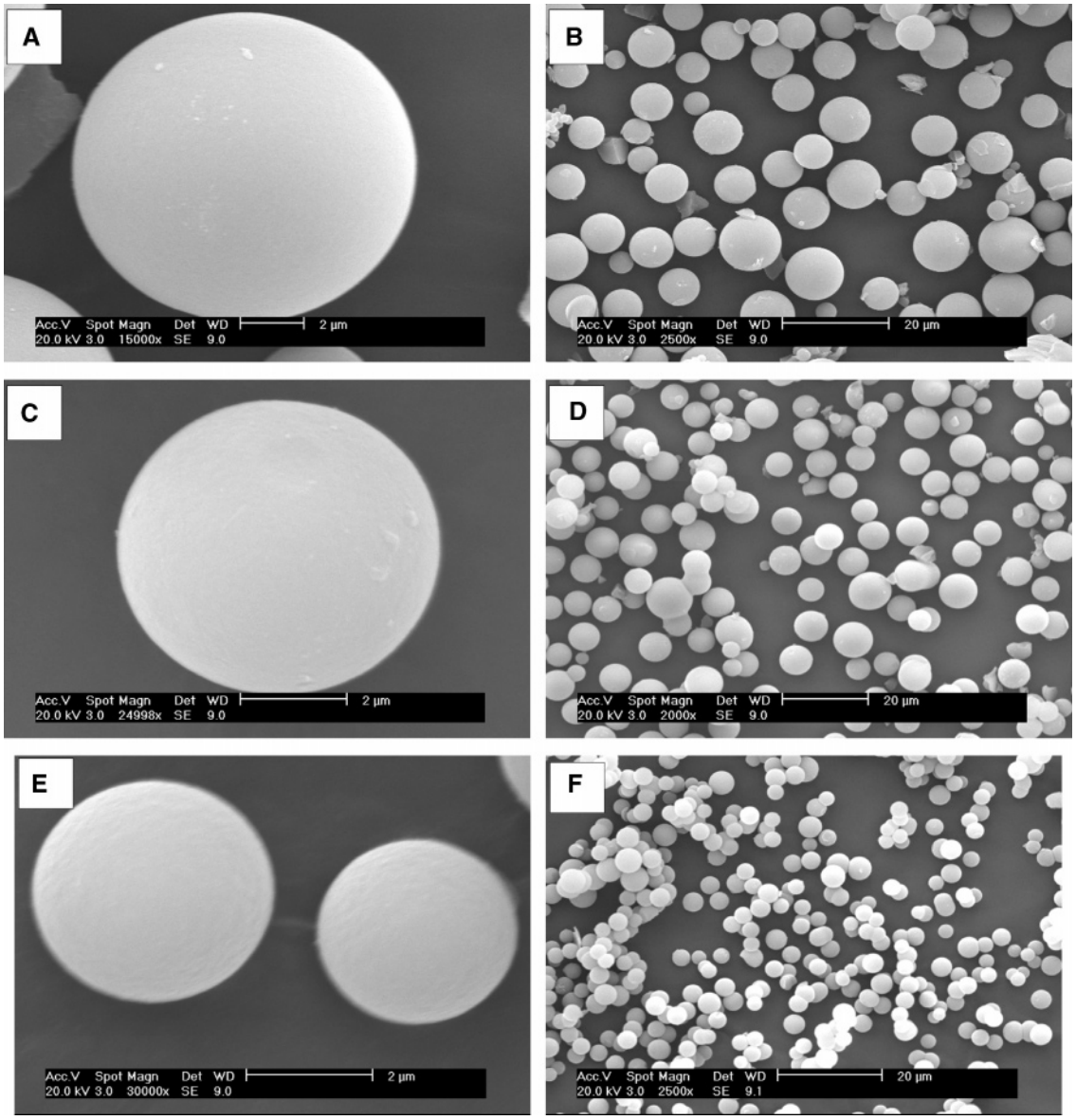

Figure 2. Representative SEM images of spherical ethylene-bridged organosilica materials synthesized at a H_2O/NaOH molar ratio of 150 and various DTAB concentrations; H_2O/DTAB molar ratio of (A and B) 600, (C and D) 300, and (E and F) 225.

branch of the isotherms was used to calculate the pore size distribution so as to avoid any ambiguities that may arise from tensile strength effects, which are known to occur at P/P_0 of between 0.4 and 0.5 for nitrogen sorption at −196 °C.)[16]

The pore size distribution curves in Figure 4 indicate that the spherical PMOs have relatively uniform pore size distribution. Although the isotherms of samples EHOI-A, -B, and -C suggest a slight bimodal pore structure, the pore size distribution over a wide size range (Supporting Information Figure 2S) did not show evidence of there being a significant proportion of pores of sizes above 30 Å. The PSD curves over wide pore size ranges (Supporting Information Figure 2S) therefore confirmed that the porosity of the PMOs is dominated by pores in the size range of 20−25 Å, although there is a contribution from pores in the range of 40−60 Å. The larger pores may arise from defects in the pore ordering or from interparticle voids (textural mesoporosity). The presence of these larger pores would, however, be an asset in the use of the PMO spheres as stationary phases in chromatographic applications. The pore wall thickness of the PMO materials can be estimated from the basal spacing and pore size. The wall thickness was calculated as the difference between the lattice parameter a_o ($a_o = 2d_{100}/\sqrt{3}$), and the pore size varies between 20 and 25 Å.[10c] Such thick pore walls are advantageous with respect to the mechanical stability of the PMO spheres especially for applications as the stationary phase in liquid-phase chromatography.

The surface area (>900 m^2/g) and pore volume (>0.8 cm^3/g) of the spherical PMO materials are relatively high and typical for well-ordered MCM-41 type mesoporous materials.[15] It is noteworthy that all the organosilica materials have comparable textural properties (Table 1). This suggests that even those samples that exhibit rather poor XRD patterns are still highly porous and possess some mesostructural ordering. Furthermore, nitrogen sorption isotherms of organosilica spheres synthesized at various H_2O/DTAB molar ratios (Figure 5) indicate that despite differences in sphere size (Figure 2), the spherical PMOs have comparable mesostructural ordering. Indeed, the textural properties in

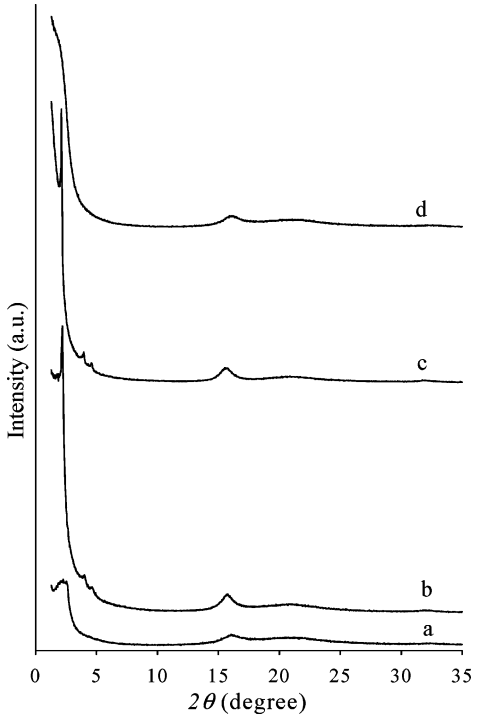

Figure 3. Powder XRD patterns of ethylene-bridged organosilica materials prepared at a H_2O/DTABr molar ratio of 300 and varying basicity at a H_2O/NaOH molar ratio of (a) 225, (b) 200, (c) 180, and (d) 163.6.

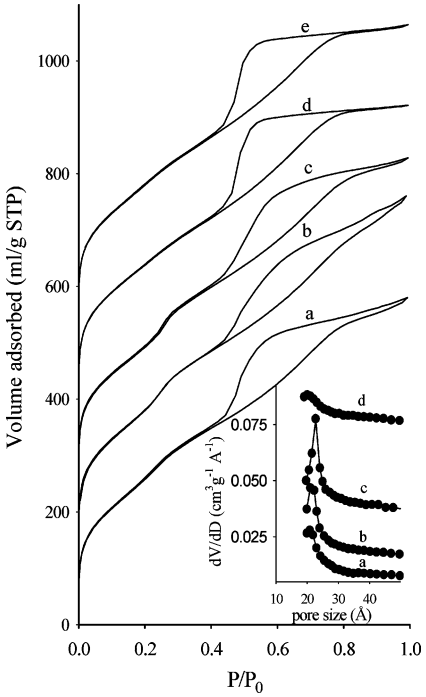

Figure 4. Nitrogen sorption isotherms of ethylene-bridged mesoporous organosilica materials prepared at a H_2O/DTABr molar ratio of 300 and varying basicity at a H_2O/NaOH molar ratio of (a) 225, (b) 200, (c) 180, (d) 163.6, and (e) 150. For clarity, isotherms b−e are offset (*y*-axis) by 120, 240, 380, and 500, respectively. The inset shows the corresponding pore size distribution curves. Curves b−d are offset (*y*-axis) by 0.01, 0.03, and 0.07, respectively.

Table 1 show that the surface area and pore volume of samples EHOI-E, -F, and -G are similar. This confirms that despite the changes in sphere size, the surface area, pore volume, and pore diameter of the spherical PMOs remain largely unaffected.

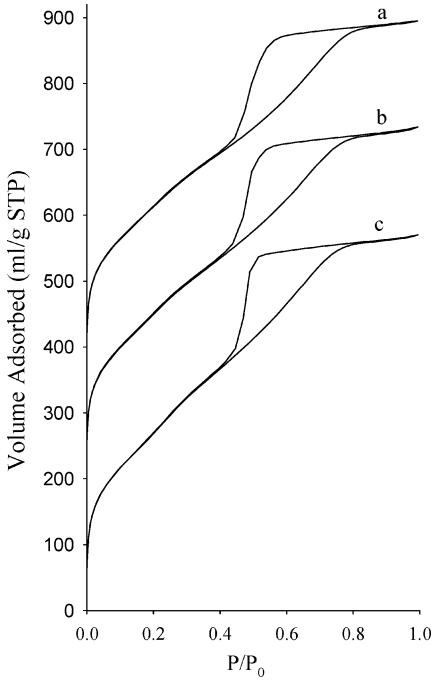

Figure 5. Nitrogen sorption isotherms of ethylene-bridged mesoporous organosilica spheres synthesized at a H_2O/NaOH ratio of 150 and various H_2O/DTAB molar ratios (a) 600, (b) 300, and (c) 225. For clarity, isotherms a and b are offset (*y*-axis) by 300 and 150, respectively.

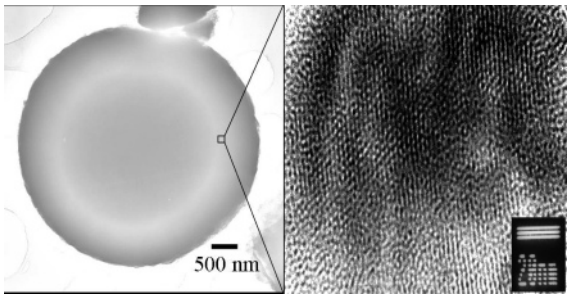

Figure 6. Representative TEM image of spherical periodic mesoporous organosilica (sample EHOI-C) showing a well-formed sphere and a high level of pore channel ordering.

The structural ordering of the ethylene-bridged PMO spheres was also evidenced by transmission electron microscopy (TEM) as shown by the representative TEM image in Figure 6. Well-ordered pore channels are clearly observed for sample EHOI-C, indicating good pore channel mesostructural ordering. From the TEM image, it is possible to estimate a pore channel diameter of 2.2 nm, which is similar to the pore size obtained from nitrogen sorption studies (Table 1). The information from the TEM image therefore confirms that the pore size of the PMO spheres is ca. 2.2 nm. This agreement between TEM analysis and porosity data is important given that the determination of pore size using BJH analysis of nitrogen sorption data has a number of limitations.[16]

Si-C Binding and Reactivity of Ethylene Groups; Functionalization of C═C Bond. ^{29}Si and ^{13}C MAS NMR was used to probe the Si−C binding in the mesoporous organosilica spheres. Representative ^{29}Si and ^{13}C MAS NMR spectra for the materials (sample EHOI-C) are shown in Figure 7. The ^{29}Si MAS NMR spectrum of surfactant extracted sample EHOI-C (Figure 7A, top) exhibits two main signals at −74.5 and −83.6 ppm. The signals are assigned

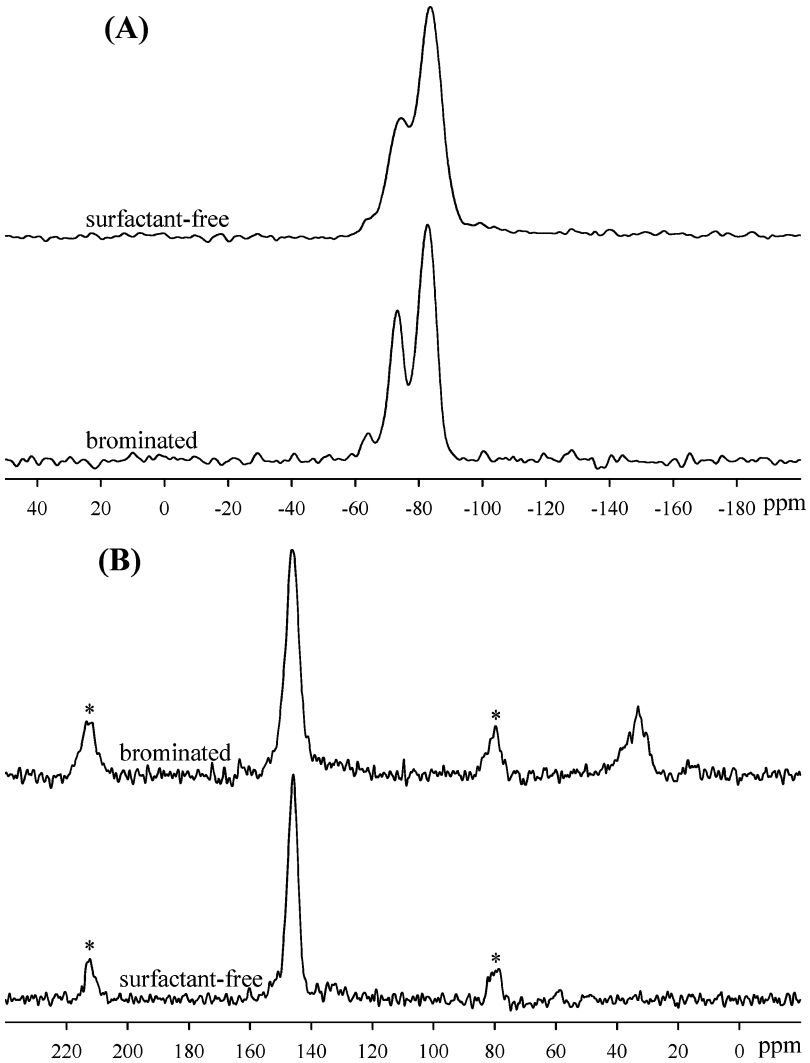

Figure 7. Representative ^{29}Si MAS NMR (A) and ^{13}C MAS NMR (B) spectra of spherical ethylene-bridged mesoporous organosilica (sample EHOI-C) before and after bromination. (Asterisk denotes a spinning sideband.)

to silicon bonded to carbon (i.e., T^2 [C−SiO_2(OH)] at −74.5 ppm and T^3 [C−SiO_3] at −83.6 ppm). Q^n[(Si(OSi)$_n$(OH)$_{4-n}$), $n = 2-4$] peaks in the range −90 to −115 ppm were not observed, confirming that carbon−silicon cleavage of the BTEE species did not occur during synthesis of the organosilica spheres. The relative intensity of the T^n peaks suggests that ca. 70% of the Si in the materials is in the T^3 environment. The ^{13}C NMR spectrum (Figure 7B, bottom) displays a main peak at ca. 146 ppm due to ethylene (−CH═CH−) functional groups linked to silicon. It is worth noting that the ^{13}C NMR spectrum exhibits no significant peaks in the range of 10−30 ppm, which gives a clear indication that virtually all the surfactant was removed from the organosilica samples during the template extraction process.

To probe the reactivity and/or accessibility of the ethylene groups, we performed bromination experiments on sample EHOI-C. We first note that bromination did not have any significant influence on the mesostructural ordering of the organosilica material; the low-angle region of XRD patterns and nitrogen sorption isotherms is relatively similar before and after bromination (Supporting Information Figure 3S). However, as expected the surface area, the pore volume and pore size decrease after bromination (Table 1). The pore size decrease from 22.7 to 20.6 Å is consistent with previous reports on brominated ethylene-bridged PMOs.[10a,10c,12c,13c] However, bromination significantly reduced the molecular scale periodicity of the ethylene groups; the intensity of the peak at $2\theta = 16.5°$ was much lower for the brominated sample (Supporting Information Figure 3S). The decrease in intensity of the peak at $2\theta = 16.5°$ may simply be a result of disruption of the ethylene functional groups after reaction with bromine to generate C−Br bonds. Bromination did not affect the spherical particle morphology (Supporting Information Figure 4S), except perhaps for an apparent increase in the surface roughness. The bromination had little effect on the Si environments as shown by the ^{29}Si NMR spectrum of the brominated sample in Figure 7A. As expected, the ^{13}C NMR spectrum of the brominated sample (Figure 7B) exhibits a peak at ca. 33 ppm, which arises from carbon−bromine (C−Br) bonds. This peak confirms that a proportion of the ethylene groups in the spherical mesoporous organosilica is accessible to functionalization. It is noteworthy that both carbon atoms in ethylene groups turn to chiral carbons after bromination, which may present an alternative route for the preparation of mesoporous organosilica materials with chiral carbon centers.[17] It is therefore possible that due to the versatile reactivity of ethylene groups, chiral carbons can

be readily formed, thus extending the range of potential PMO applications into chiral catalysis and separation. The retention of the −CH═CH− peak (at 146 ppm) in the ^{13}C NMR spectrum of the brominated sample (Figure 7B) is consistent with the wide-angle XRD patterns (Supporting Information Figure 3S) and confirms that under our reaction conditions, not all the molecularly ordered ethylene groups react with the bromine.

Conclusions

In summary, ethylene-bridged mesoporous organosilica spheres, of sizes between 3 and 14 μm, were successfully synthesized via surfactant-mediated assembly of BTEE without using any additional cosolvents and/or cosurfactants. The resulting mesoporous spheres exhibit molecular-scale periodicity (due to ethylene groups) in the organosilica framework. The ethylene groups present a versatile functionality that can be readily subjected to further chemical modification. This means that new properties such as chirality (of the ethylene carbons) may be introduced into the mesoporous organosilica spheres. The morphology and structural ordering of the ethylene-bridged mesoporous materials can be easily adjusted by controlling the basicity of the synthesis media. In particular, the PMO sphere sizes may be tuned from 3 to 14 μm via simple changes in the concentration of surfactant in the synthesis gel mixtures. The flexibility exhibited by the ethylene-bridged mesoporous materials presented here, namely, molecular-scale periodicity, good mesostructural ordering, reactive and readily functionalized organo groups, and relatively monodisperse sphere morphology with tunable sphere sizes, is attractive and likely to find use in a variety of applications including multifunctional catalysts, macromolecule separations, drug delivery, and particularly as the stationary phase in liquid-phase chromatography.

Acknowledgment. This work was funded by EPSRC and the University of Nottingham. The authors thank Dr. David Apperley at the EPSRC Solid State NMR service (Durham) for the NMR spectra.

Supporting Information Available: Four additional figures, low-angle region powder XRD patterns of mesoporous organosilicas, pore size distribution curves of mesoporous organosilica materials over wider pore size ranges, powder XRD patterns, nitrogen sorption isotherms, and SEM images of mesoporous organosilica materials before and after bromination. This information is available free of charge via the Internet at http://pubs.acs.org.

CM0526563

(17) (a) Che, S.; Liu, Z.; Ohsuna, T.; Sakamoto, K.; Terasaki, O.; Tatsumi, T. *Nature* **2004**, *429*, 281. (b) Moreau, J. J. E.; Vellutini, L.; Man, M. W. C.; Bied, C. *J. Am. Chem. Soc.* **2001**, *123*, 1509.